Electromagnetics, Heat Transfer, and Thermokinetics in Microwave Sterilization

H. Zhang and A. K. Datta
Dept. of Agricultural and Biological Engineering, Cornell University, Ithaca, NY 14853

I. A. Taub and C. Doona
U.S. Army Natick Soldier Center, Natick, MA 01760

Sterilization of solid foods using microwave power was studied using numerical modeling and specialized experimental verification. Maxwell's equations and the heat conduction equation were coupled using two separate finite-element programs and specially written modules to couple the programs. Spatial distributions of thermal-time, representing sterilization, were calculated from time-temperature history and first-order kinetics. Experimentally, concentrations of marker compounds formed during heating were measured and taken as indices of thermal-time. Experimental data on marker formation combined with numerical calculations provide an accurate and comprehensive picture of the sterilization process and represent a major step in establishing the efficacy of microwave sterilization processing. Unlike conventional sterilization, heating patterns can change qualitatively with geometry (shape and size) and properties (composition) of the food material, but optimal heating is possible by choosing suitable combinations of these factors. Combined with marker yield measurements, the numerical model can give comprehensive descriptions of the spatial time-temperature history, and thus can be used to verify the sterilization process.

Introduction

In the sterilization of foods and biomaterials, undesirable changes such as loss of nutrients accompany the desired destruction of bacteria. However, many of the undesired changes are less sensitive to temperature as compared to the bacterial destruction. Thus, a higher temperature and shorter time process has long been recognized as preferred, that is, one that would destroy the microorganisms in a short time, while compromising relatively less of the desired attributes and components, such as nutrients. The difficulty with a higher-temperature-shorter time process is the practical limitation on reaching a high temperature quickly. The long come-up time in conventional retorting often destroys a significant amount of desired components. Microwaves offer a unique opportunity to raise the temperature quickly without the heat diffusion limitations, thus lowering thermal destruction of components during the come-up time. However, the nonuniformities in the spatial distribution of energy deposition during microwave heating and the changes in distribution during the heating process can be distinctly different from conventional retort heating. This study describes a comprehensive understanding of the process using modeling and experimental verification.

Microwave sterilization has been a subject for research (Heddleson and Doores, 1994; Mudgett and Schwartzberg, 1982; Schlegel, 1992), as well as for potential commercial application (Harlfinger, 1992). However, its commercialization has been plagued by several issues (Schiffmann, 1992) and very few systems are in use commercially (Tops, 2000). Simply having one or a few temperature readings during the microwave heating is not enough to provide a complete thermal picture of the process, because the heating patterns can be uneven, difficult to predict, and changing during heating. Hence, researchers of microwave sterilization have reached inconsistent, even conflicting, conclusions about the effectiveness and advantages of microwave processing over conventional methods (Heddleson and Doores, 1994), due to a lack

Correspondence concerning this article should be addressed to A. K. Datta.

of comprehensive information on the time-temperature history.

The ability of microwaves to reduce thermal degradation of quality attributes and components is not universally true and depends on a number of food and oven factors. Food factors, such as dielectric properties, size, and shape, play more important roles as compared to conventional retorting, because they affect not only the magnitude of heat generation, but also its spatial distribution. As the food is heated, its dielectric properties and in turn change the microwave absorption process. This change in properties changes the heating patterns qualitatively, unlike conventional retorting where the qualitative nature of the heating remains unchanged even as thermal properties change during heating. Thus, microwave sterilization would involve coupled electromagnetic and thermal studies. A complete picture of microwave sterilization involving coupled thermal-electromagnetic studies with a comprehensive experimental verification of the computations has not been previously reported. It is the intended objective of this study to present such a picture.

Coupled solutions of Maxwell's equations in a cavity (such as the domestic microwave oven) and of the energy equation in 3-D, which is fundamentally necessary for the study of microwave sterilization, is computationally demanding and only few studies have been reported. Solutions of Maxwell's equations for simplified special cases have been presented (Ayappa et al., 1992; de Pourcq, 1983; Paoloni, 1989; Webb et al., 1983). More general solutions of Maxwell's equations for a 3-D cavity have been reported, (Zhang and Datta, 2000; Burfoot et al., 1996; Torres and Jecko, 1997; Fu and Metaxas, 1992; Ma et al., 1995; Ohlsson and Risman, 1993; Zhao and Turner, 1996). Only a few of these have coupled electromagnetics with the energy equation (Zhang and Datta, 2000; Burfoot et al., 1996; Torres and Jecko, 1997; Ma et al., 1995), but, with one exception (Zhang and Datta, 2000), did not elaborate on the effect of the changes in properties during heating on the spatial distribution of the electromagnetic field patterns. These coupled studies also did not cover temperatures high enough for sterilization, where temperatures greater than 121°C are reached, often starting from room temperature. Such a large temperature change for some materials (such as foods with significant water and ionic contents) can cause very significant changes in heating (and sterilization) patterns during the heating process. This is a special feature of the microwave sterilization process and can only be studied by strongly coupling the electromagnetics and heat transfer.

Considerable spatial and time-dependent nonuniformity of heating is possible during microwave heating and, if not properly considered, could effectively limit the commercialization of the microwave sterilization process. This potential for nonuniformity in the sterilization process has not been comprehensively described. A powerful descriptor of the integrated time-temperature effect and its spatial variations is the "thermal-time distribution" (Nauman, 1977; Datta and Liu, 1992), which has not been used in the context of microwave sterilization. For such sterilization processes to be accepted commercially and approved by the regulatory authorities, it is required that the thermal-time distributions in these processes be understood and verified. This can be achieved very effectively through a computational study of the coupled heat transfer and electromagnetics, combined with experimental verification of the thermal-time distributions.

One direct way to verify the thermal-time or sterility would be to spatially sample the processed material and to analyze for bacterial concentration, but it is cumbersome and fraught with major difficulties (Prakash et al., 1997). An alternative is the use of intrinsic chemical markers that are formed during the heating process due to the reaction between protein and ribose or glucose (Kim and Taub, 1993; Prakash et al., 1997). Measured marker yields can comprehensively verify the calculated thermal-time distribution and, together with the computational results, can provide insight into the process and confidence in the development of successful microwave sterilization processes.

The specific objectives of this study are:

(1) To develop a numerical model that couples the electromagnetics, heat transfer, and first order, bacterial-destruction and marker-formation kinetics to predict temperatures and thermal-time distributions during a sterilization process.

(2) To comprehensively verify the model's predictions of the thermal-time distributions during sterilization using the experimental measurement of intrinsic chemical marker formation during the heating process.

To develop insight into the changes in heating and sterilization patterns as they unfold during the heating process as a function of food properties.

Mathematical Formulations

Governing Maxwell's equations and boundary conditions

The microwave heating system with the cavity and a cylindrical food is shown in Figure 1. The food is placed inside a

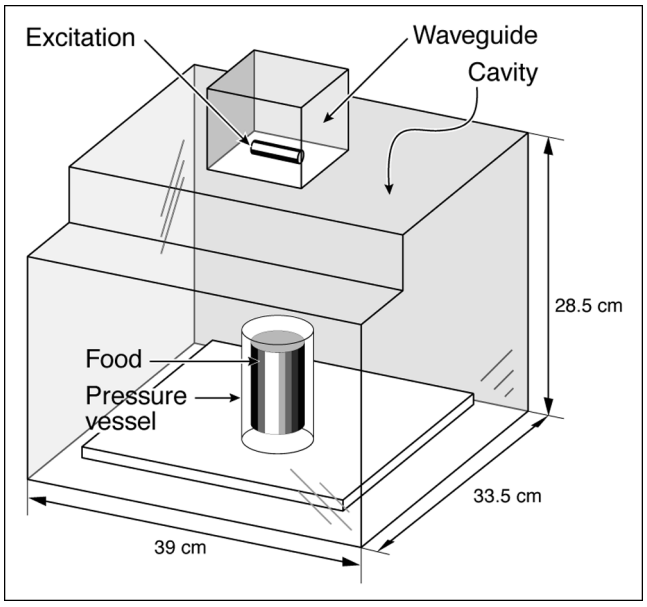

Figure 1. CEM microwave oven and pressure vessel.

The mode stirrer normally in the microwave oven was removed.

pressure vessel in order to reach the high temperatures needed for sterilization. Since high pressure developed in the vessel stops further evaporation, changes in water content of the sample are considered small and are neglected in this study. Microwave reflection and transmission inside the cavity and the foods are described by the Maxwell's equations

$$\nabla \times \boldsymbol{E} = j\omega\mu\boldsymbol{H} \tag{1}$$

$$\nabla \times \boldsymbol{H} = -j\omega\epsilon_0\epsilon^*\boldsymbol{E} \tag{2}$$

$$\nabla\cdot(\epsilon\boldsymbol{E}) = 0 \tag{3}$$

$$\nabla\cdot\boldsymbol{H} = 0 \tag{4}$$

where $\boldsymbol{E}$ and $\boldsymbol{H}$ are the time-harmonic electric and magnetic fields, respectively. The complex permittivity, ϵ^* is given by

$$\epsilon^* = \epsilon' + j\epsilon''_{eff} \tag{5}$$

The cavity and waveguide walls are metallic and can be considered as perfect electric conductors, where the following boundary condition applies

$$E_{\text{tangential}} = 0 \tag{6}$$

The excitation of the microwave power is treated as sinusoidal at 2.45 GHz (domestic microwave oven frequency) given by

$$I = I_0 \sin(\omega t) \tag{7}$$

The microwave power absorption or heating potential in food, $P(\boldsymbol{r}, \boldsymbol{T})$, is related to the electric fields by

$$P(\boldsymbol{r}, T) = \frac{1}{2}\omega\epsilon_0\epsilon''_{\text{eff}}\boldsymbol{E}^2 \tag{8}$$

This absorbed energy causes the food temperature to rise.

Governing heat conduction equation and boundary conditions

The uneven volumetric heat generated by microwaves $P(\boldsymbol{r}, T)$ diffuses inside the food and is convected into the surrounding air, which is typically colder. This process is described by the transient heat equation

$$\rho C_p\frac{\partial T}{\partial t} = \nabla\cdot(k\nabla T) + P(\boldsymbol{r}, T) \tag{9}$$

Inside the microwave oven, air flows at a low velocity over the pressure vessel, leading to the boundary condition

$$-k\nabla T = h(T - T_{\text{air}}) \tag{10}$$

where h is mainly due to free convection on the pressure vessel surfaces as the sample warms up. There is a small air flow inside the cavity due to a small fan outside the cavity, leading to a small h. In this study, h is assumed to be 5 W/m^{2}K (see analysis in Zhang and Datta, 2000). The initial temperature of the food is assumed uniform

$$T = T_i \tag{11}$$

For most bio-materials including foods, heat generation is a nonlinear function of temperature due to the changing dielectric properties. As the material is heated, its dielectric properties change, which in turn changes at a particular location the electric field that causes the heat generation. Thus, a solution has to couple the Maxwell's equation (Eqs. 1 to 4) with the heat conduction equation (Eq. 9). Since E in Eq. 8 changes during the process, it is obvious that the set of nonlinear coupled partial differential equations needs to be solved numerically.

Kinetics of marker formation and sterilization

The spatial temperature variations arising during microwave heating described in the previous sections lead to spatial variation of the time-temperature history and thus of the consequent thermal effects on microorganisms, nutrients, and any other biochemical reactions, which are now discussed.

Sterilization. During sterilization, our concern is the destruction of spore-forming microorganisms from a safety standpoint and the degradation of nutrients and sensory attributes from a quality standpoint. These destruction and degradation rates are usually described as first-order reactions, and can be written for bacterial destruction as

$$-\frac{dc}{dt} = k_b c \tag{12}$$

where c is the concentration of a food component at time t, and k_b is the reaction rate constant. The rate constant is a function of temperature T, generally assumed to follow the Arrhenius Law

$$k_b = k_0 e^{-\frac{E_{a,b}}{RT}} \tag{13}$$

where k_0 is called the frequency factor, $E_{a,b}$ is the activation energy for the bacterial destruction, and R is the universal gas constant. The solution to Eq. 12 is given by

$$\ln\frac{c_i}{c} = k_0\int_0^t \exp(-E_{a,b}/RT)\,dt \tag{14}$$

Instead of referring to a final concentration c, food technologists use an equivalent heating time F_0 that provides the same final concentration when the temperature T is constant at a reference temperature T_R (usually chosen as 121°C). Using this definition, F_0 can be derived as

$$F_0^b = \frac{\ln(c_i/c)}{k_{b,T_R}} = \frac{k_0 \int_0^t \exp(-E_{a,b}/RT)dt}{k_0 \exp(-E_{a,b}/RT_R)} = \int_0^t \exp\left[\frac{E_{a,b}}{R}\left(\frac{1}{T_R} - \frac{1}{T}\right)\right]dt \quad (15)$$

where $E_{a,b}$ is the activition energy for *Clostridium botulinum* (Lund, 1975). From a food microbiological safety consideration, the lowest value of F_0^b anywhere in food of this pathogenic spore-former needs to be above a certain value. When this is true, the food is considered commercially sterile.

Marker Formation. Direct experimental verification of the bacterial destruction F_0^b (Eq. 15) poses challenges (Kim and Taub, 1993). Instead, intrinsic chemical markers whose extent of formation is a function of the time-temperature history have been used to verify such effects (Kim and Taub, 1993). For example, the reactions between proteins and ribose or glucose yield distinctive and detectable chemical compounds. Measured spatial distribution of these chemical markers can be compared with the numerically calculated thermal-time (Eq. 15) obtained from electromagnetic and thermal modeling.

Formation of intrinsic chemical markers are described as first-order reactions given the assumption of an excess source of either the protein or ribose/glucose precursor in food materials (Kim and Taub, 1993; Ross, 1993)

$$\frac{dM}{dt} = k_m(M_\infty - M) \quad (16)$$

where M is the concentration of intrinsic chemical marker at time t, M_∞ is the maximum amount of marker formed after extensive processing, and k_m is the rate constant at a particular temperature. The solution to this equation for an initial marker concentration of zero can be written as

$$\frac{M}{M_\infty} = 1 - \exp\left(-k_{m,T_R}F_0^m\right) \quad (17)$$

where F_0^m is calculated in a similar way as Eq. 15 with $E_{a,b}$ for bacterial destruction replaced by $E_{a,m}$ for marker formation

$$F_0^m = \frac{\ln((M_\infty - M)/M_\infty)}{k_{m,T_R}} = \int_0^t \exp\left[\frac{E_{a,m}}{R}\left(\frac{1}{T_R} - \frac{1}{T}\right)\right]dt \quad (18)$$

Since both the marker formation defined by Eq. 17 and the bacterial destruction defined by Eq. 15 depend on the time-temperature history in the same manner, verification of the calculated marker formation using experimental measurements is analogous to verification of bacterial destruction in sterilization (Ross, 1993). Conceptually, a correspondence can be established between F_0^b and F_0^m values. In this study, the concentration of marker formation M obtained from experimental measurement is compared with computations of the same quantity using the mathematical model.

Input parameters

Tables 1 and 2 list the numerical values for the parameters used in the simulations. Dielectric properties of the food materials as functions of temperature, taken from the work of Romaine and Barringer (1998), will be shown in Figure 6. Temperature variation in dielectric loss factor is stronger at higher salt content where ionic effects dominate. The thermal conductivity and specific heat of the two materials, whey protein and ham, used in the experiments increase slightly with temperature (Rahman, 1995). Their values are extrapolated beyond 100°C in this study due to lack of available data. Normally, at high temperature (up to 130°C), food thermal properties follow the trend observed under 100°C (Gratzek and Toledo, 1993).

Microwave power absorbed by the load is a function of the microwave system (Figure 1), including size and geometry of the cavity and the power source (as modeled by the excitation probe), locations of the wave entry port, amplitude of the excitation current (I_0), and the dielectric properties of the

Table 1. Parameter Values Used in the Calculations

Parameter	Whey Protein Gel	Ham	Source
Radius, cm	1.45	1.45	
Height, cm	6	6	
$\epsilon' + j\epsilon''$	$46.3 + j17.3$	Figure 6	Romaine and Barringer (1998)
ϵ_0, F/m	8.854×10^{-12}	8.854×10^{-12}	
μ_0, H/m	$4\pi\times10^{-7}$	$4\pi\times10^{-7}$	
f, GHz	2.45	2.45	
T_i, °C	20	20	This study
T_{air}, °C	23	23	This study
I_0, A	0.595	0.595	This study
T_R, °C	121	121	Lund (1975)
ρ, kg/m^3	1 100	1 390	Rahman (1995)
c_p, J/kg·K	$4.032 + 0.00146T$	$0.541 + 0.00135T$	Rahman (1995)
k_t, W/m·K	$3.49 + 0.00146T$	$0.449 + 0.00135T$	Rahman (1995)
h, W/m^2·K	5	5	This study
k_m (M-2), /min	0.12 (at 121°C)		Doona et al. (2000)
$E_{a,m}$, kJ/mol	89.25		Doona et al. (2000)
k_m (M-2), /min		0.316	Prakash and Taub (2000)
$E_{a,m}$, kJ/mol		103.07	Prakash and Taub (2000)
M, initial value	0	0	
k_b (C-bot), /min	10.97 (at 121°C)	10.97	Lund (1975)
$E_{a,b}$, kJ/mol	290.01	290.01	Lund (1975)

Table 2. Properties of Teflon and Plexiglass*

Parameter	Teflon	Plexiglass
$\epsilon' + j\epsilon''$	$2.1 + j0.00063$	$3.45 + j0.138$
k_t, W/m°·C	0.024	0.052
ρ, kg/m^3	1 427	1 121
c_p, J/kg·K	1 372	1 078

From "Aries Material Property Database" by MacNeal-Schwendler Corporation (1998).

load (food). All other factors remaining constant, the power absorbed by the load is a function of the excitation current, I_0, as discussed in detail in Collin (1991) and Weeks (1964). For this study, I_0 is estimated from the experimental power absorbed by a water load as obtained from its temperature rise.

Numerical Solution

Microwave system

Figure 1 shows the microwave cavity, waveguide, food, and pressure vessel. The microwave oven used in this research is MDS-2000 Microwave Digestion System (CEM Corp., Matthews, NC). Using the programmable control system of the oven with a fiber optic temperature sensor (Figure 2), a sterilization temperature of 121°C can be reached and maintained in the pressure vessel containing the food. The transient temperature data is stored.

The pressure vessel is made of Teflon having 5 mm wall thickness. Between the food sample and pressure vessel, there is a plexiglass layer as shown in Figure 2. The dielectric loss factors of Teflon and plexiglass are small (Table 2), so that the pressure vessel and plexiglass do not absorb significant amounts of power. However, they affect the heating pattern of a food sample inside due to their large dielectric constants (see Figure 7 later).

The dimensions shown in Figure 1 are used in the numerical simulations. The microwave source is modeled as an excitation probe that carries alternating current at a frequency of 2.45 GHz. Along with the waveguide, the excitation can account for the reflected power from the cavity (for details, see Zhang and Datta, 2000). Thus, the model can be used to quantify the relative power absorptions by different loads.

Coupling methodology

The governing equations were solved using finite-element methods. Two commercial FEM software packages were used — EMAS (Ansoft Corporation, Pittsburgh, PA) for electromagnetic fields and NASTRAN (MacNeal-Schwendler Corporation, Los Angeles, CA) for temperature distributions. Coupling is not built into the software, and system level codes were written in C language to develop the two way coupling, as shown in Figure 3. Additional details of the coupling process are not included here and the reader is referred to Zhang and Datta (2000). The computational time was about 6 h of cpu time for each run of electromagnetics and about 0.5 h for each run of heat transfer on a HP 9000, model 735 workstation.

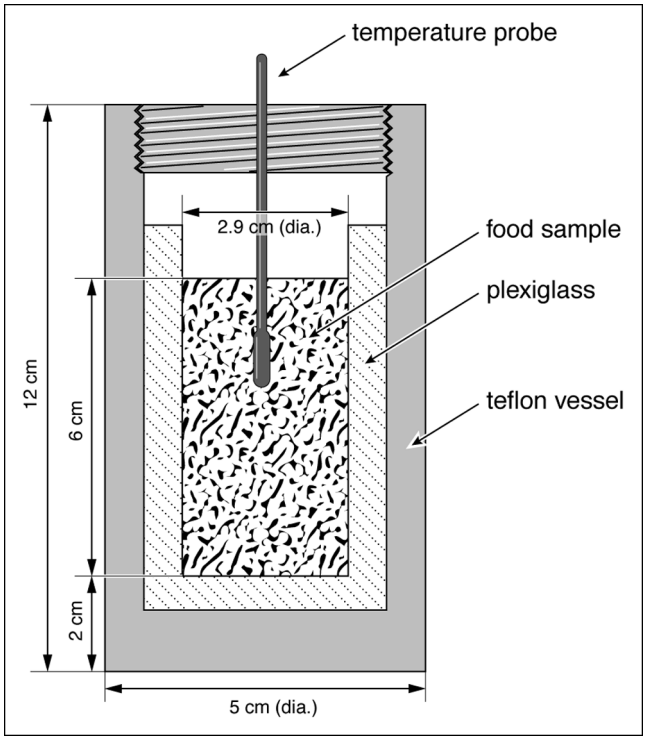

Figure 2. Pressure vessel, plexiglass layer, and food sample.

Convergence study

Figure 4 shows how one of the solution variables (total energy absorbed) changes as mesh size is reduced. Without losing much accuracy, a mesh size criterion of 3 mm between nodes is selected in the software for the meshes generated in this study. Note that 3 mm is approximately the maximum distance between nodes, although a small number of elements can be larger. Choices of this mesh size criterion is necessarily a compromise, otherwise the computation time can be significantly longer. An acceptable criterion for the finite-element solution of Maxwell's equations for a plane wave has been shown to require six nodes per wavelength (MacNeal, 1990). In a cavity, however, the wavelengths are not unique, since multiple modes are resonated. Nevertheless, a 3 mm distance between nodes was considered a compromise between accuracy and excessive computing time.

Comparison with experimental marker yields

As explained earlier, the measured marker yield from a first-order formation reaction is treated as representative of sterilization. Marker formation is calculated using Eq. 17 for every finite element in the sample. The computational results are compared with experimental marker measurements, in which samples are divided into the six sections as shown in Figure 5. An average value of computed marker formation in each of the six sections is calculated as

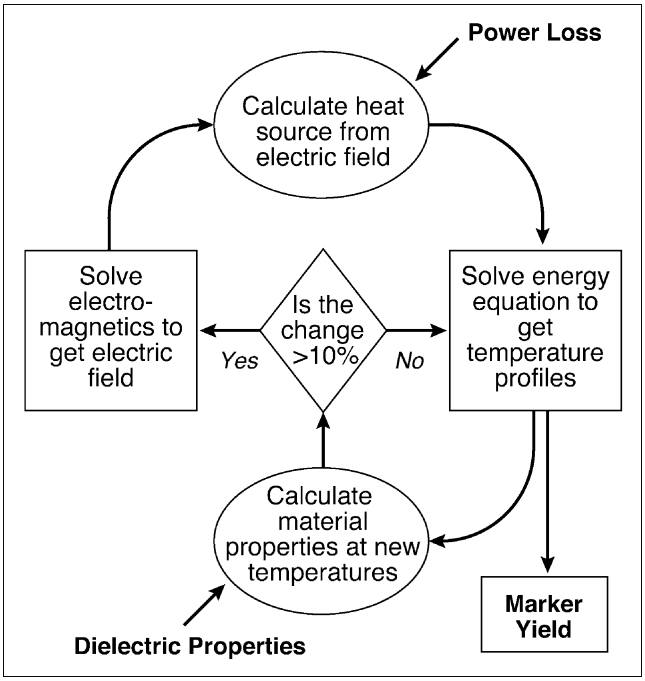

Figure 3. Coupling of electromagnetic and thermal calculations.

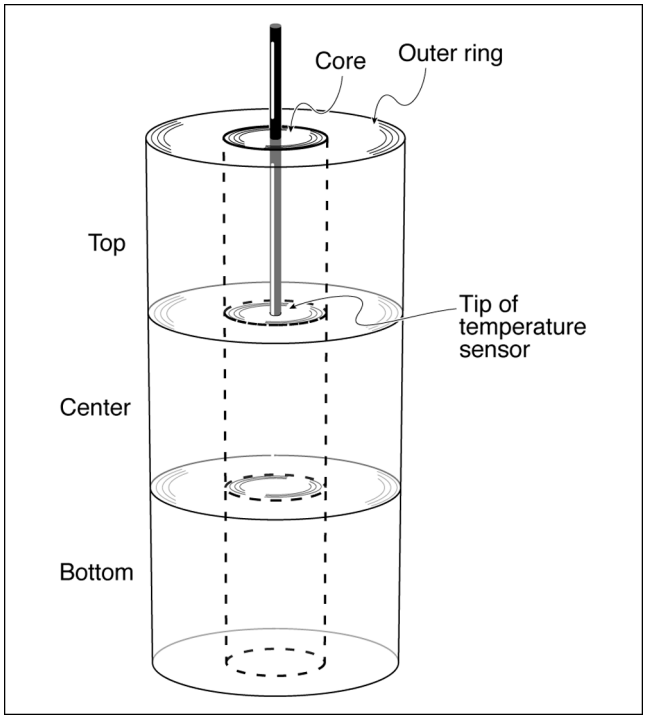

Figure 5. Sectioning of the cylindrically shaped food sample in Figure 2 for marker analysis.

Six sections comprise of the top, center and bottom of the core and outer ring, respectively. The fiber optic temperature sensor is positioned at 1/3 height from the top.

$$\overline{M} = \frac{1}{v_0} \sum_{i=1}^{n} M_i v_i \tag{19}$$

where v_0 is the total volume of the section, v_i is the volume of ith element, and n is the total number of elements in the section.

Calculation of thermal time and its spatial distribution (volume fraction curves)

The numerical model calculates the thermal time F_0 using Eq. 15 using the average temperature for each finite element. The small size of a typical element (0.03 cm^3) should lead to a sufficiently accurate calculation of the spatial distribution of thermal time values. Since thermal time is a continuous variable over the entire spatial domain of computation, it is presented as a volume fraction curve following the procedure developed by Datta and Liu (1992). Such a volume fraction curve provides information on the volume fraction of the food material that has the thermal time in a particular range. Like thermal time, temperature is a continuous variable as well, and volume fraction curves will also be used to represent the fraction of food material in a particular temperature range.

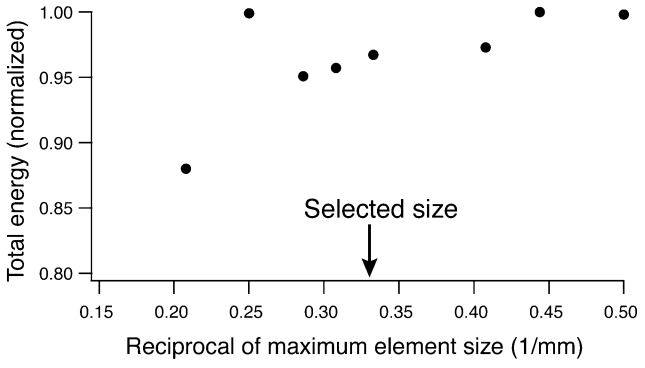

Figure 4. Convergence of the electromagnetic calculations as the mesh is refined.

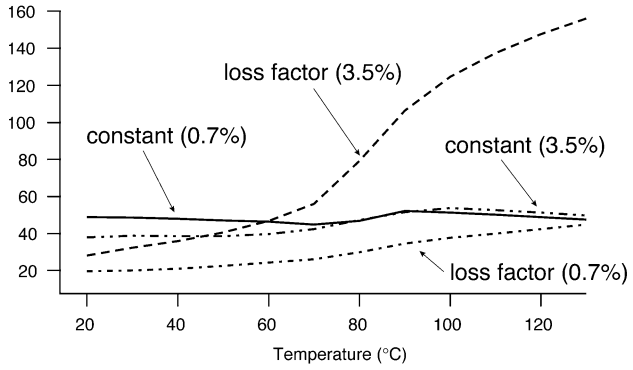

Figure 6. Dielectric properties of ham with 0.7% and 3.5% salt contents.

From Romaine and Barringer (1998).

Experimental Procedure

Sample preparation

A solution containing 20% whey protein concentrate (Alacen 878, from New Zealand Milk Product, Santa Rosa, CA), 1% ribose, and water was heated in a water bath at 80°C for 45 min. The resulting gel was cut into cylinders of diameter 1.45 cm and height 6 cm. The ham material was specially prepared to control the uniformity and salt content, as well as the moisture level. Two days before the experiments, ham was injected with 1% ribose, which is added to enhance the M-2 marker yields (see Kim and Taub (1993) for details about marker M-2). It is assumed that during this time period the ribose will diffuse to a uniform concentration throughout the sample. The ham was also cut into the same shape and size as the whey protein gel.

Temperature measurement and control during microwave heating

Temperature is measured using a fiber optic temperature sensor that is inert to the microwaves. The sensor is placed in the sample, as shown in Figure 5. Samples are heated in the microwave oven starting from room temperature. The microwave power level is varied from 10% to 40% of the full power (630 W). To reduce the temperature overshooting and increase the heating uniformity, the heating duration is divided into three stages, as detailed in Table 3. Towards the end of stage 2, the probe temperature reaches approximately the target temperature of 121°C (the time to reach this temperature is considered the come-up time), and further temperature control at ± 2°C around the target temperature during stage 3 is achieved by automatically turning the microwaves on and off. Heating is continued for another four minutes or so, which is considered 121°C exposure time.

Following the microwave treatment, the pressure inside the vessel is released by unscrewing the lock nut, which reduces the temperature immediately to less than 100°C. The sample is removed and immediately (within ten seconds) sectioned for marker analysis.

Measurements of marker yields

About one gram of material from a randomly selected location within a section (Figure 5) is homogenized with four times as much volume of water using a Polytron (Brinkman Instruments, Westbury, NY), centrifuged and filtered through a 0.45 micron nylon membrane filter. The amount of marker in this aqueous extract is measured by anion exclusion chromatographic (AEC) separation and photodiode array (PDA) detection. The AEC-PDA system comprises a Wescan (Deerfield, IL) anion exclusion column and a Waters 990 PDA detector (Milford, MA). The eluant used is a 10 mM sulfuric acid solution and the flow rate is 1 mL/min. The marker concentrations are obtained in relative terms by integrating the area under the respective elution peaks and the data are stored in a computer. Further details of marker yield measurement can also be seen in Kim and Taub (1993).

Table 3. Stages of Microwave Heating to Control the Sample Temperature at Target Values*

Stage	Power Level: Whey Protein Gel	Power Level: Ham	Target Temp. (°C)	Programmed Time at Targeted Temp. (s)
1	40%	30%	60	30
2	30%	20%	90	90
3	20%	10%	121	240

*Note that the actual heating duration for each stage is automatically adjusted by the control system to reach the targeted temperature.

Results and Discussions

Temperature and marker yields, computed numerically and measured experimentally, are presented in this section for the microwave heating of whey protein gel and ham samples. Thus, the calculated marker yields refer to the use of Eq 16. The calculated values are normalized by dividing them by the maximum value at that time for that sample. The experimentally measured marker yields are also normalized by dividing them by the maximum of the experimental values at that time for that sample. Effects of property changes on the sterilization process are described using volume fraction curves of temperature and thermal-time F_0.

Electric field distributions

An example of computed field distributions in the pressure vessel assembly containing a food sample is shown in Figure 7. As expected, electric fields in the food sample are generally lower than the vessel because of higher dielectric constant. Even though high electric fields exist in the vessel, there is very little energy loss due to the small dielectric loss factor of Teflon.

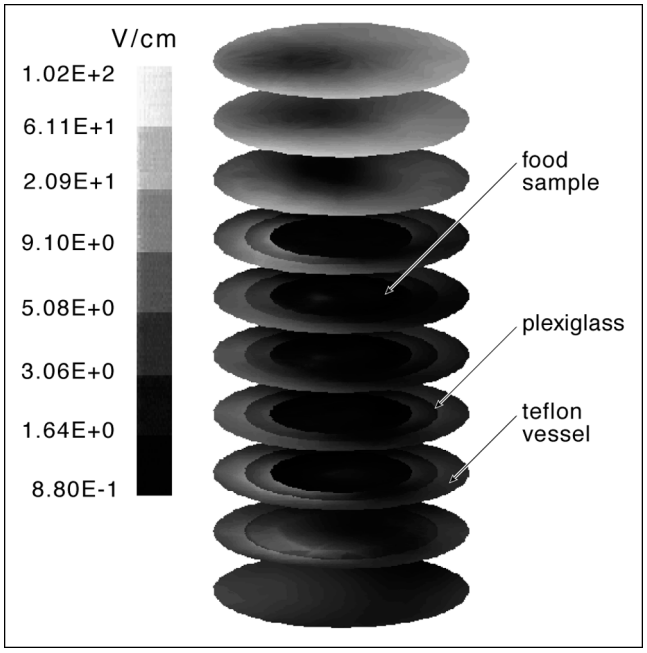

Figure 7. Electric fields in food sample, plexiglass, and teflon vessel for the assembly in Figure 2 during heating stage 1 of 0.7% salt ham.

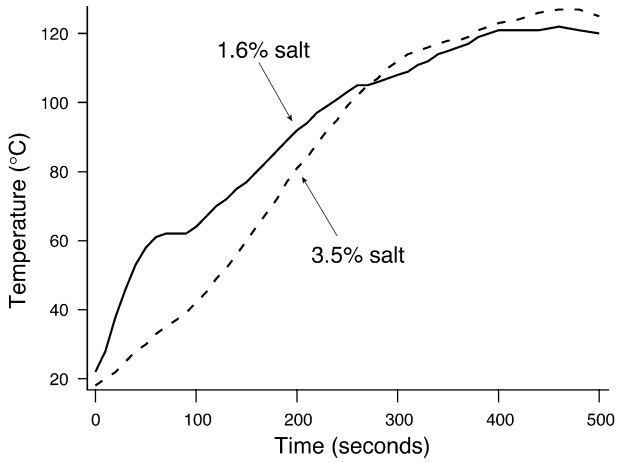

Figure 8. Probe temperature history for ham with two different salt levels.

Different stages of heating are described in Table 3.

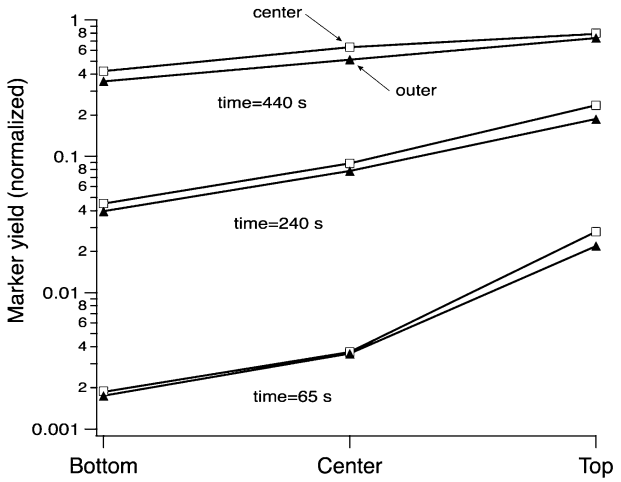

Figure 9. Calculated increase in M-2 marker yields for whey sample during sterilization.

Shown for the center and outer rings of the bottom, center, and top sections, the yields being normalized to the maximum attainable.

Temperature history during microwave heating

Temperature history for the probe location in Figure 5 is shown in Figure 8 for two materials with different lossiness (ham with two different salt contents). The plateau in the temperatures are caused by the heating stages, as shown in Table 3. The faster heating of a less lossy material (ham with 1.6% salt content) during the initial stages in Figure 5 can be explained by the focusing effect of microwaves. The curved cylindrical surface of the food can focus the microwaves at interior locations, much like a lens focusing the light waves. However, the higher loss factor of the 3.5% salt content ham prevents much of the microwave energy from reaching the center (counterbalancing the focusing effect), making the temperature at the center increase slower. As heat gradually diffuses from outside warmer locations to colder inside, probe temperature rises to 127°C even after the microwaves are turned off (Table 3) at 121°C by the controller. Therefore, the probe temperature is only representative of the immediate vicinity and not indicative of other locations unless the overall heating pattern due to the significant spatial variation is elucidated (discussed later).

Changes in sterilization during come up and holding times

Based on calculations of M-2 formation, the first 65 s of heating produces only a very small yield of marker, as shown in Figure 9, due to the low temperatures. By the time the temperature exceeds 100°C ($t = 240$s), the marker yields become substantial, reflecting 5–15% conversion of precursors. After further heating ($t = 440$s), which includes holding at 121°C, the yields of marker reach high levels. The distribution of marker yields at much later times is also more uniform, but by then the maximum yield would be reached as the precursors are completely depleted (Kim and Taub, 1993).

Spatial distributions of sterilization

Spatial distributions of the numerically predicted and experimentally measured marker yields are shown in Figures 10, 11 and 12 for three different materials (whey protein gel, ham with 0.7%, and 3.5% salt contents, respectively). The higher concentrations of markers in the center compared with the outer region in these figures indicate focusing of the microwaves for lower loss materials (whey protein gel and 0.7% salted ham). This effect is not seen in Figure 12 in the heating of high loss material (3.5% salted ham). The model predictions agree with experimental data very well (Figures 10, 11, and 12). The experimental and numerical data are also in agreement in predicting significantly more heating in the up-

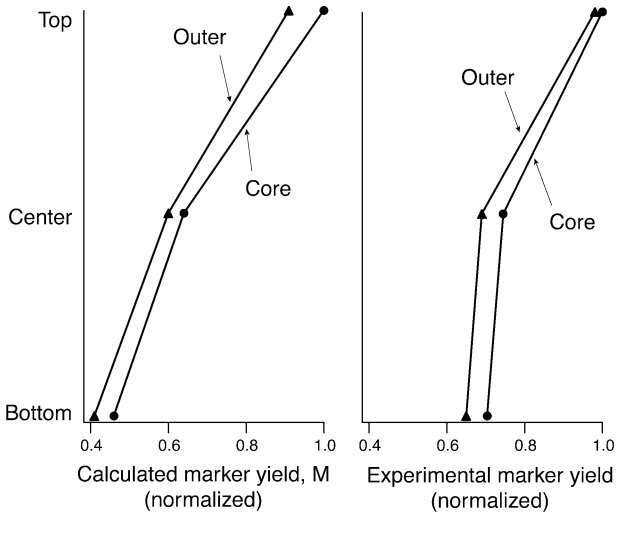

Figure 10. M-2 marker yields from numerical prediction: (a) with experimental measurement; (b) for whey protein gel with a cylindrical geometry in Figure 5.

The total duration of heating is 550 s following the protocol in Table 3. Marker yields are normalized relative to the top core yield in each case.

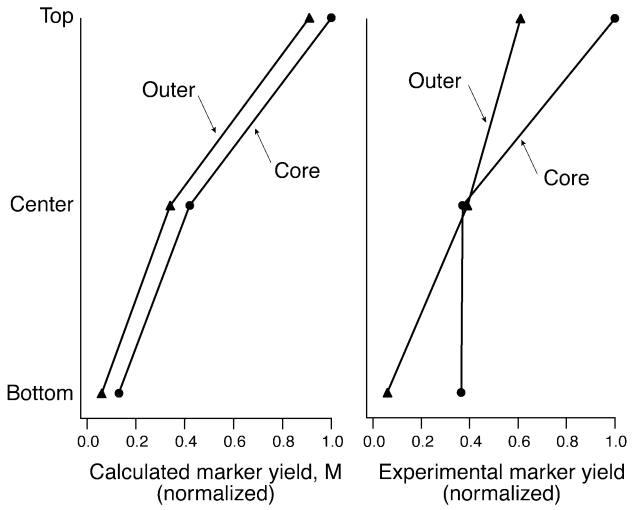

Figure 11. M-2 marker yields from numerical prediction: (a) experimental measurement; (b) for ham with 0.7% salt, normalized relative to the top core yield in each case.

The total duration of heating is 480 s following the protocol in Table 3.

per part of the cylinders. Consistently higher heating at the top of the samples indicates that the cavity standing wave pattern is not significantly changed by the material properties of the different loads. It can be concluded that the overheating at the top of the cylindrical load is mainly associated with the sample location in this specific cavity (Figure 1), as the same location is used for the three cases.

There are, however, some differences between model predictions and experimental data. For example, the measured

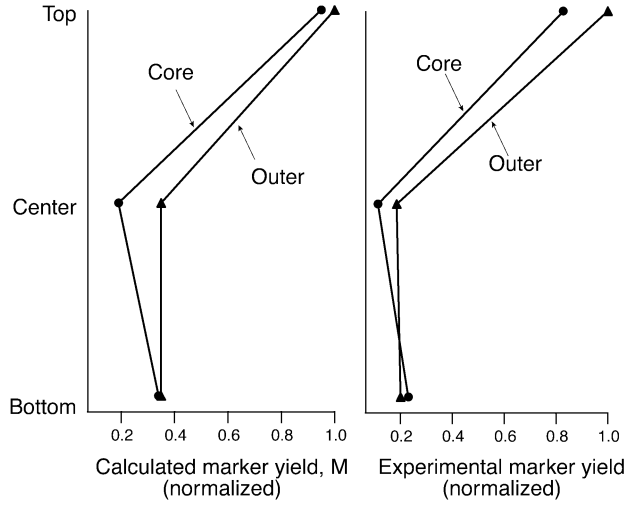

Figure 12. M-2 marker yields by numerical prediction: (a) experimental measurement (b) for ham with 3.5% salt, normalized relative to the top outer yield in each case.

The total duration of heating is 486 s following the protocol in Table 3.

values at the bottom for whey protein gel are higher than that of the predictions (Figure 10), and the marker yields at the bottom outer location for 0.7% salted ham are much lower than that of the predicted ones (Figure 11). The nonuniform distribution of added ribose in the sample might account for the lower yield at the bottom outer region in the 0.7% salted ham. Alternatively, water released from the sample at high temperature drains down and could move some marker to the bottom of the sample (and even out of the sample into the vessel itself).

Effect of property on the unifomities of temperature and sterilization

One way to quantify heating nonuniformity is to use the standard deviation T_{nu} defined by

$$T_{nu} = \sqrt{\int_{\text{vol}} T^2 dv_f - \left(\int_{\text{vol}} T dv_f\right)^2} \tag{20}$$

where v_f is the volume fraction of the material at temperature T. Figure 13 shows this nonuniformity for three materials with different loss, after six minutes of cumulative heating. The nonuniformity is highest for low loss material (ham at the low salt concentration) due to the focusing effect and for high loss material (ham with the highest salt content) due to the decreased penetration and increased surface heating. It is lowest for the ham with 1.6% salt content. Thus, improvement in uniformity can be achieved by manipulating the dielectric properties by changing composition for a compromise between focusing in the center and preferential surface heating. However, the heating differences between the upper and the lower parts of the samples (Figures 11 and 12) due to the cavity heating pattern are not alleviated by changing the dielectric properties (salt contents).

The volume fraction curves (as discussed earlier) for temperature for ham with different salt levels are plotted in Figure 14. The curves show that the range of temperatures

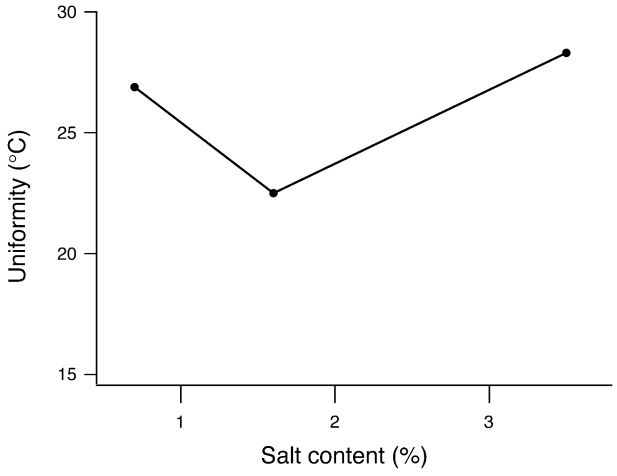

Figure 13. Uniformity of temperatures T_{nu} for ham with different salt levels.

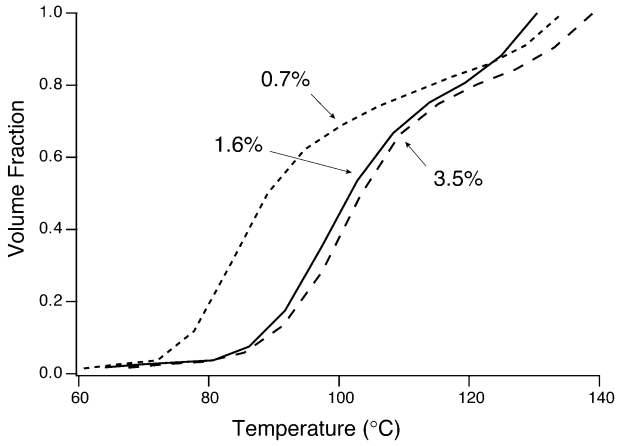

Figure 14. Calculated volume fraction curves for temperature in ham with salt contents of 0.7%.

1.6%, and 3.5% after 500 s of microwave treatment.

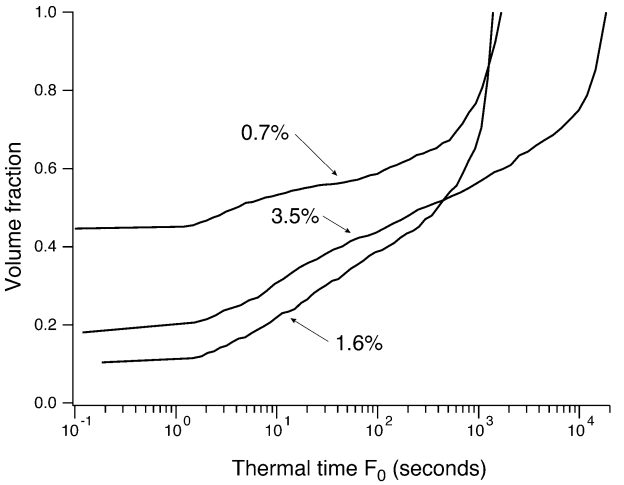

Figure 15. Calculated volume fraction curves for thermal time F_0 (bacteria) in ham with salt contents of 0.7%, 1.6% and 3.5% after 500 s of microwave treatment.

(characterizing the nonuniformity of heating) is the smallest for 1.6% salt. The hottest 10% of the volume (fraction between 0.9 and 1.0) has a higher average temperature for the 3.5% salt, as compared to the other two salt concentrations, representing overheating at the edges at this higher salt content. Likewise, the coldest 10% of the volume (fraction between 0.0 and 0.1) has a lower average temperature for the 0.7% salt compared to the other two salt concentrations, representing more underheating. These curves lead to the conclusion that an appropriate salt content could be chosen, such as 1.6% for the size and shape of ham in this study, for which the sterilized food material will have fewer overheated and underheated volumes. However, it should be noticed that the differences due to different salt contents are not overwhelming, since the cavity heating patterns and edge overheating effects are not altered by the content of salt.

A more comprehensive way to quantify and improve our understanding of the sterilization process is by using volume fraction curves for thermal-time or F_0 (concept of thermal-time distribution, as proposed by Nauman (1977) and used in Datta and Liu (1992). The thermal time (Eq. 15) is analogous to residence time, but accounts for the temperature history. Calculated volume fraction curves for thermal time for bacteria are shown in Figure 15 for samples having three different dielectric properties after 500 s of cumulative heating. Analogous to Figure 14, in Figure 15 the volume fraction for a certain thermal-time represents the portion of the material below that thermal time. For the low loss material (0.7% salt ham samples), large volume fraction (about 60%) of material falls in the low thermal-time range (below $F_0 = 6$ min), indicating that the material is underheated, that is, the thermal time is below the desired minimum of $F_0 = 6$ min. For a high loss material (ham with 3.5% salt content), over 40% of material exceeds 2,000 s thermal time (above $F_0 = 33$ min), representing significant overheating (that is, thermal time much above the desired $F_0 = 6$ min) in the outer ring. Intermediate lossy (ham with 1.6% salt) material gives a better thermal time distribution and shows the smallest range of thermal time, even though the range, from 0.1 to 1200 s, is still quite large due to the nature of the cavity heating.

It should be noted that the nonuniformity described here represents perhaps a worse case scenario for this cavity corresponding to a load that is centrally located in the cavity and kept fixed in that location. Considerable improvement in uniformity was attained in this cavity by placing ham samples 12 cm off-center and rotating them in the horizontal plane. Industrial implementation of microwave sterilization would need to pay attention to various means of improving the uniformity of electric field patterns in designing the cavity.

Need for coupled solutions

Since the dielectric properties are temperature sensitive, the distribution of electric fields, defined as heating potential, changes with the heating time. The initial distribution of heating potential, as shown in Figure 16a, changes as heating progresses (Figure 16b). The distribution of initial heating potential is different from that during the later heating time. The focusing effect (that is, hotter locations are inside), which is initially present, is not significant after the material reaches the sterilizing temperature (when the hotter locations move to the surface). This qualitative and significant change in heating pattern has to be taken into consideration in the calculations of marker yields by coupling the electromagnetics with energy transfer in microwave sterilization.

Conclusions

(1) A coupled thermal-electromagnetic model was combined with kinetics to describe microwave sterilization in a comprehensive way. Coupling of heat transfer and electromagnetics was necessary to account for significant changes in dielectric properties during heating. The model predictions were verified by obtaining experimental data involving chemical marker yields that are functions of time-temperature history in the material.

(2) The time-temperature history and thus the sterilization vary spatially in a very significant way. Additionally, the

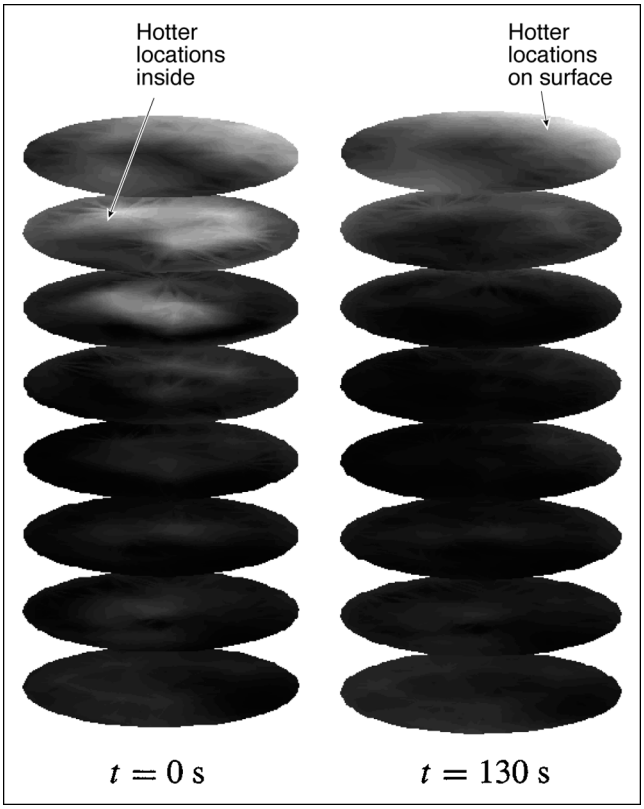

Figure 16. Horizontal sections of cylindrical food at equal vertical intervals showing the change in heating potential from initial time to after 130 s of continuous heating.

Lighter shades of gray represent increased magnitude of heating potential.

time-temperature history changes qualitatively during heating, changing the relative spatial variation in sterilization. The spatial nonuniformity of sterilization and its transient changes can be improved significantly by changing the material's dielectric properties, which are a function of its composition. Effect of salt content was found to be particularly pronounced.

(3) Information on the least thermal-time and its location is of primary importance for the microbial safety of sterilized food. Since heating patterns can change dramatically for different food materials, different placements in the oven, and different oven designs, and, since the patterns can also change during heating, a combination of a coupled thermal-electromagnetic model complemented with experimental measurement of marker formation are needed for a comprehensive and verifiable picture of microwave sterilization.

Acknowledgment

We acknowledge the financial support by the U.S. Army Natick Soldier Center at Natick, MA. This research was also partly supported by the USDA NRI program with grant No. 94-37500-0586. We appreciate the high temperature dielectric property data provided by Prof. S. Barringer of The Ohio State University.

Notation

c = mass concentration, kg/m^3
c_p = specific heat, J/kg·K
E = electric field, V/cm
$E_{a,b}$ = activation energy for microorganism, kcal/mol
$E_{a,m}$ = activation energy for marker, kcal/mol
F_0 = thermal time at 121°C, min
h = convective heat transfer coefficient, W/m^2·K
H = magnetic field, A/cm
I = current, A
k_b = rate constant for marker formation
k_t = thermal conductivity, W/m·K
k_0 = frequency factor
k_m = rate constant for destruction of microorganisms
k_{b,T_R} = rate constant for marker formation at reference temperature
k_{m,T_R} = rate constant for microorganisms at reference temperature
M = marker concentration
P = microwave power density or heating potential, W/m^3
R = universal gas constant, J/kmol·K
$\boldsymbol{r}$ = position vector
t = time, s
T = temperature, °C
T_{nu} = nonuniformity, °C
T_R = reference temperature, °C
v = volume, m^3

Greek letters

ϵ = permittivity F/m
ϵ_0 = permittivity in air F/m
ϵ^* = complex permittivity F/m
ϵ' = dielectric constant
ϵ'' = dielectric loss
ϵ''_{eff} = effective dielectric loss
ρ = apparent density of the food, kg/m^3
ω = angular frequency
σ = electric conductivity, S/m
μ = magnetic permeability, H/m

Literature Cited

Ayappa, K. G., H. T. Davis, E. A. Davis, and J. Gordon, "Two-Dimensional Finite Element Analysis of Microwave Heating," *AIChE J.* **38** 1577 (1992).

Burfoot, D., C. J. Railton, A. M. Foster, and R. Reavell, "Modeling the Pasteurisation of Prepared Meal with Microwave at 896 MHz," *J. of Food Eng.*, **30**, 117 (1996).

Collin, R. E., *Field Theory of Guided Waves*, IEEE Press, Piscataway, NJ (1991).

Datta, A. K., and J. Liu, "Thermal Time Distributions for Microwave and Conventional Heating of Food," *Trans. IChemE*, **70**:83 (1992).

de Pourcq, M., "Field and Power-Density Calculations by Three-Dimensional Finite Elements," *IEEE Proc.*, 130, 377 (1983).

Doona, C., M. Lau, J. Tang, and I. Taub, "Kinetics of Marker Formation," unpublished data (2000).

Fu, W., and A. Metaxas, "A Mathematical Derivation of Power Penetration Depth for Thin Lossy Materials," *J. of Microwave Power and Electromag. Energy* 27, 217 (1992).

Gratzek, J. P. and R. T. Toledo, "Solid Food Thermal Conductivity-Determination at High Temperatures," *J. of Food Sci.*, **58**, 908 (1993).

Harlfinger, L., "Microwave Sterilization," *Food Technol.* **46**, 57 (1992).

Heddleson, R., and S. Doores, "Factors Affecting Microwave Heating of Foods and Microwave Induced Destruction of Foodborne Pathotens: a Review," *J. of Food Protection*, **57**, 1025 (1994).

Kim, H.-J., and I. A. Taub, "Intrinsic Chemical Markers for Aseptic Processing of Particulate Foods," *Food Technol.*, **47**, 91 (1993).

Lund, D., "Heat Processing," *Principles of Food Science*, O. R. Fennema, ed., Marcel Dekker, New York (1975).

Ma, L., D. Paul, N. Pothecary, C. Railton, J. Bows, L. Barratt, J. Mullin, and D. Simons, "Experimental Validation of a Combined Electromagnetic and Thermal FDTD Model of a Microwave

Heating Process," *IEEE Trans. on Microwave Theory and Techniques*, **43**, 2565 (1995).
MacNeal, B. E., "Permittivity (Mass) Discretization for Best Accuracy," *MSC/EMAS RF and Microwave Technical Notes* 4, 1 (1990).
Mudgett, R., "Electromagnetic Energy and Food Processing," *J. of Microwave Power and Electromag. Energy*, **234**, 225 (1988).
Mudgett, R. E., and H. G. Schwartzberg, "Microwave Food Processing: Pasteurization and Sterilization—a Review," *AIChE Symp. Ser.* **78**, 1 (1982).
Nauman, E. B., "Nonisothermal Reactors: Theory and Applications of Thermal Time Distributions," *Chem. Eng. Sci.*, **32**, 359 (1977).
Ohlsson, T., and P. Risman, "Temperature Distribution in Microwave Oven Heating—the Influence of Different Cavity Modes," T. Yano, R. Matsuno, and K. Nakamura, eds., *Int. Cong. on Food and Eng.*, (ICEF 6th International Congress on Eng. and Food), 1–7 Chiba, Japan, Blackie Academic and Professional (inprint of Chapman and Hall), Glasgow, U.K. (1993).
Paoloni, F., "Calculation of Power Deposition in a Highly Overmoded Rectangular Cavity with Dielectric Loss, *J. of Microwave Power and Electromag. Energy*, **24**, 21 (1989).
Prakash, A., H.-J. Kim, and I. A. Taub, "Assessment of Microwave Sterilization of Foods Using Intrinsic Chemical Markers," *J. of Microwave Power and Electromag. Energy*, **32**, 50 (1997).
Prakash, A. and I. A. Taub, "Kinetics of Marker Formation," unpublished data (2000).
Rahman, S., "Food Properties Handbook," CRC Press, Boca Raton, FL (1995).
Romaine, A. and S. A. Barringer, "Dielectric Properties of Ham as a Function of Temperature, Moisture and Salt," *Inst. of Food Technologists Meeting*, Atlanta, IFT, Chicago, IL (1998).
Ross, E. W., "Relation of Bacterial Destruction to Chemical Marker Formation during Processing by Thermal Pulses," *J. of Food Eng.* 16, 247 (1993).
Schiffmann, R. F., "Microwave Processing in U.S. Food Industry," Food Technology, **46**, 12, 50 (1992).
Schlegel, W., "Commercial Pasteurization and Sterilization of Food Products Using Microwave Technology," *Food Technol.*, **46**, 62(1992).
Tops, R., "Industrial Implementation: Microwave Pasteurized and Sterilized Products," *Symp. on Microwave Sterilization, IFT Meeting*, Dallas, TX, IFT, Chicago, IL (2000).
Torres, F. and B. Jecko, "Complete FDTD Analysis of Microwave Heating Processes in Frequency-Dependent and Temperature-Dependent Media," IEEE Trans. on Microwave Theory and Techniques, **45** 108 (1997).
Webb, J. P., G. L. Maile, and R. L. Ferrari, "Finite Element Solution of Three Dimensional Electromagnetic Problems," *IEE Proc.*, **130**, 153 (1983).
Weeks, W. L., *Electromagnetic Theory for Engineering Applications*, Wiley, New York (1964).
Zhang, H. and A. K. Datta, "Coupled Electromagnetics and Heat Transfer of Microwave Oven Heating of Foods," *J. of Microwave Power and Electromag. Energy 35*, 71 (2000).
Zhao, H., and I. W. Turner, "An Analysis of the Finite-Difference Time-Domain Method for Modeling the Microwave Heating of Dielectric Materials within a Three-Dimensional Cavity System," *J. of Microwave Power and Electromag. Energy* **31**, 199 (1996).

Manuscript received July 9, 1999, and revision received Feb. 19, 2001.